Nat. Hazards Earth Syst. Sci. Discuss., https://doi.org/10.5194/nhess-2018-258
Manuscript under review for journal Nat. Hazards Earth Syst. Sci.
Discussion started: 19 October 2018

Natural Hazards and Earth System Sciences
Open Access
EGU
Discussions

Accuracy of geodetic site velocities from repeated GPS measurements: relative positioning over long baselines

Huseyin Duman[1] and Dogan Ugur Sanli[1]

[1]Department of Geomatics Engineering, Yildiz Technical University, Istanbul, 34220, Turkey

Correspondence: Dogan Ugur Sanli (usanli@yildiz.edu.tr)

Abstract. ~~Currently,~~ GPS campaign measurements ~~(i.e. repeated GPS measurements)~~ are used frequently in order to determine geophysical phenomena such as tectonic motion, fault zones, landslides, and volcanoes. ~~The coordinates of a new point installed in a study area are usually found either by using relative point positioning or precise point positioning (PPP).~~ Employing observation sessions shorter than 24 h might still be a necessity at times. When observation duration is shorter, the accuracy of coordinates are degraded and also the accuracy of point velocities are affected. The accuracies of the geodetic site velocities from a global network of the International GNSS Service (IGS) stations were previously investigated using only PPP. In this study, we extend that study in which site velocities will also be assessed including fundamental relative positioning. PPP derived results will also be evaluated to see the effect of JPL reprocessed products and single receiver ambiguity resolution. IGS is a good data source for simulation studies and hence globally distributed 18 continuously operating IGS stations were chosen to create synthetic GPS campaigns. GPS data were processed comparatively using GAMIT/GLOBK v10.6 and GIPSY/OASIS II v6.3. The data of synthetic campaign GPS time series were processed using a regression model accounting for the linear and seasonal variation of the ground motion. Once accepting the velocities derived from 24 hour sessions as the truth, the results from sub-sessions were compared with the results of 24 hours and hypothesis testing was applied for the significance of the differences. The major outcome of this study is that at global scales (i.e. over long distances) with short observation sessions, the fundamental relative positioning produces similar results to PPP. The reliability of the velocity estimation for horizontal components has now been improved to about 85% on the average for observation durations of 12 h.

1 Introduction

GNSS ~~technologies~~ have been widely used to monitor geophysical phenomena. Monitoring schemes have generally been conducted using either continuous (i.e. permanent GPS stations) or ~~repeated~~ GNSS measurements, ~~which are mainly controlled by the economic conditions, security reasons, logistic concerns, and etc~~. The accuracy of positioning from campaign measurements is ~~naturally poorer~~ than continuous ones due to the length of observation session (Segal and Davis, 1997). Researchers studied the effect of observation duration, baseline length, and design of reference network on the accuracy of GPS positioning (Dogan, 2007; Eckl et. al., 2001; Soler et. al., 2006; Firuzabadì and King, 2012; Sanli and Engin, 2009; Hayal and Sanli, 2016). It is significant to emphasize that the accuracy of the geodetic site velocities obtained from shorter observation sessions also need to be studied because the coarser positioning accuracy due to short session would lead to a coarser velocity accuracy.

Many studies to understand the geophysical phenomena (i.e. tectonics, faults, and volcanoes) have been carried out by different research groups or scientific societies. Various authors have studied tectonics (Floyd et. al., 2010) and point-based quality control using 24-hour GNSS data (Kenyeres and Bruyninx, 2004; Moore et. al., 2014), whereas some combined continuous data with shorter duration sessions from repeated GNSS measurements (Aktuğ et. al., 2015; Müller et. al., 2013; Reilinger et. al., 2006). There are so many experiments in the literature experiencing only the use of campaign GPS data (Aktuğ et. al., 2009, 2013; Dogan et. al., 2014; Koulali et. al., 2015; McClusky et. al., 2000; Ozener et. al., 2010; Tatar et. al., 2012). However, the fact that the estimated velocities are altered due to short observation session is clearly highlighted in (Hastaoglu and Sanli, 2011; Akarsu et. al., 2015; Duman and Sanli, 2016).

Akarsu et. al. (2015) examined the effect of campaign GPS on site velocities at global scales using PPP. Here, we extend this study in which along with PPP solutions, fundamental relative positioning solutions are also assessed and comparisons between the results of the two methods are made. Furthermore, the effect of developments such as new JPL reprocessed products and single receiver ambiguity solution which were missing in Akarsu et al. 2015 was also tested on PPP solutions. To handle this experiment a global network of 18 IGS stations were selected and the GPS data were analysed using GAMIT and GIPSY. Synthetic GPS campaigns were created from the continuous observations with 8-, 12- and 24-hour sessions. GPS data were processed for all sessions to form north, east and up campaign time series. Velocities derived from all three GPS components calculated from both 8- and 12-hours sub-sessions were compared with the velocities from 24-hours which were accepted as the truth. The differences from the truth were statistically tested and the result were interpreted.

2 Methodology

2.1 GPS Data Analysis

GPS data were downloaded in Receiver Independent Exchange (RINEX) format with 30 sec. intervals from the Scripps Orbit and Permanent Array Center (SOPAC) which is one of the data archives of the International GNSS Service (IGS) at http://sopac.ucsd.edu/. The IGS stations used in the study are demonstrated in Figure 1. First of all, to determine the horizontal velocities for each of the stations we selected three successive days in October each year for the years 2000 through 2015. Akarsu et. al. (2015) did the similar sampling using only 1 day in a year. This is the procedure followed by many of the GPS experiments using repeated surveys (Aktuğ et. al., 2009, 2013; Dogan et. al., 2014; Koulali et. al., 2015; McClusky et. al., 2000; Ozener et. al., 2010; Tatar et. al., 2012). Using 3 consecutive days here we believe we increased the reliability of the solutions. A treatment in regard to the solar activity, which was missing in Akarsu et. al. (2015), was also taken into consideration (i.e. days with kappa index ≤ 4) here. In addition, three successive days in every month were included for the processing of the vertical component. In order to model the significant annual signal on GPS heights, here we did the sampling monthly. The GPS data were segmented into sub-sessions as listed in Table 1 in order to generate the repeated GPS measurements.

The GPS data were processed with GAMIT/GLOBK v10.6 software for relative point positioning (Herring et. al., 2006a, b) and with GIPSY/OASIS II v6.3 for PPP (Zumberge et. al., 1997). Elevation cut-off angle was set to 7^o on both software.

The processing of the GPS data using GAMIT/GLOBK was conducted in three steps (Feigl et. al., 1993; McClusky et. al., 2000; Reilinger et. al., 2006; Tatar et. al., 2012; Dong et. al., 1998). At first, the loosely constrained station coordinates, atmospheric zenith delays of each points, and Earth Orientation Parameters (EOP) were estimated using doubly differenced GPS phase measurements and IGS final products. Secondly, Kalman Filter was performed using EOP values, orbit data, the estimated station coordinates, and their covariance in order to estimate the point coordinates and velocities from the combined solution. In the last step, the reference frame was realized on each day using a reliable set of IGS stations used according to ITRF2008 no-net-rotation (NNR) frame (Altamimi et. al., 2012).

The processing strategies described above were applied to each subset of sessions listed in Table 1. The coordinate values for all sub-sessions were transformed to the topocentric system consisting of East, North, and Up. The time series of the site ZIMM from relative positioning and PPP solutions for all sub-sessions were illustrated in Figure 2.

2.2 Velocity Estimation and Statistical Tests

In this section, with the motivation from Akarsu et. al. (2015), the estimation of an IGS site velocity and the related statistical tests will be explained. In Figure 2, the comparison of all sub-session coordinate time series for all three GPS baseline components from both software results have been shown. Once looking at the time series, all sub-sessions get along well with each other. For the horizontal components that are East and North, the variations are almost perfectly linear, and this shows us the tectonic motion clearly. To estimate the linear variation (i.e. the velocity) the model of

$$x_i = a.t_i + b + o_i.x_{off} + v_i \tag{1}$$

was used. There x_i represents any coordinate value, a site velocity, t_i the time, b the intercept, and v_i the residuals. In a GPS solution time series there are additional terms such as to clarify the sudden displacements due to earthquakes. Then, Eq. (1) is expanded to include an offset value x_{off} and the corresponding coefficient o_i (Montillet et. al., 2015). For instance in our analysis, the stations AREQ and USUD include offset values in their time series due to earthquakes. For all stations, the velocity estimations were calculated using Eq. (1) by means of the least square estimation.

The vertical component additionally includes significant seasonal variation. The coordinate time series for vertical components contain repeating annual cycle stemming from hydrological and atmospheric loading (Blewitt and Lavallée, 2002). Santamaría-Gómez et. al. (2011) noticed seasonal motions in smaller periods like 3 and 4 months and diminishing amplitudes in GPS time series from continuously operating stations . Given these circumstances, it is not sufficient to determine vertical velocities with a linear model. The seasonal model we use here take into account the annual and semi-annual periodicities;

$$x_i = a.t_i + b + o_i.x_{off} + \sum_{n=1}^{q}[c_n.cos\frac{2\pi.t_i}{T_n} + d_n.sin\frac{2\pi.t_i}{T_n}] + v_i \tag{2}$$

where $q = 2$, $T_1 = 1$ year and $T_2 = 0.5$ year. The use of the offset parameter is the same as in the horizontal assessment. Furthermore, R^2 value known as “coefficient of determination” was computed in regression analysis as a statistical tool, which shows how well the data fit to the model estimated. For any coordinate component from a regression analysis, computation of R^2 is given with;

$$R^2 = 1 - \frac{\sum_{i=1}^{n} v_i^2}{\sum_{i=1}^{n} (x_i - \overline{x})^2} = 1 - \frac{\sum_{i=1}^{n} (x_i - \tilde{x})^2}{\sum_{i=1}^{n} (x_i - \overline{x})^2} \tag{3}$$

where v_i denotes residuals based on the least square estimation and $\overline{x}$ the arithmetic average of n number of measurements used in the estimation. The velocity estimation results and R^2 values from both processing strategies for the station of ZIMM have been listed in Table 2. Almost all R^2 values of the horizontal components in Table 2 for both software are at the level of 0.99 whereas those of the vertical ones range from 0.27 to 0.49. It is because the up component sampled using monthly data is not obviously linear. Parallel to the low R^2 values, the estimated velocities also fluctuate larger for the vertical component.

For all the stations in the IGS network, the solutions from sub-sessions were compared with the solutions (i.e. velocities) of 24 hours accepted as the truth. The statistical assessments of hypotheses were carried out in three steps. Then, the equivalancy between the unit variance derived from LSE of the sub-session given in Table 1 and with that of the 24h session was tested. The relevant hypothesis testing was set to be $H_0 : \sigma_{24}^2 = \sigma_s^2$ and $H_A : \sigma_{24}^2 \neq \sigma_s^2$ where σ^2 represents the unit variance and subscripts represent the observation session. A hypothesis testing based on F-distribution was applied to check the equivalancy of the variances. In the case unit variances were found to be equivalent, Student's t test was applied whether or not the velocity estimated from the campaign GPS significantly differs from the velocity derived from continuous GPS. The null hypothesis was set to be ($H_0 : a_{24} = a_s$) against the alternative hypothesis ($H_0 : a_{24} \neq a_s$) where a_i denotes the velocity values in Eq. (1) and (2). Briefly, it was tested whether or not there is a significant difference between the results of 24 hour solutions and those of the sub-sessions. In these statistical tests, the degree of freedom values for the horizontal components where approximately 42 whereas the degree of freedom for the vertical component was about 345. The degree of freedom varied with respect to the number of insignificant parameters from the LSE.

3 Results and Discussion

As described in the previous section, the time series generated from all sessions of each continuous GPS site were analyzed. The coefficient of determination (i.e. R^2), which shows how well the data fits to the model, is computed according to Eq. (3). Tables 3, 4 and 5 compare the results of sub-sessions with those of the 24-hour statistically. Tables generally consist of two columns, which includes the relative evaluation results from GAMIT / GLOBK v10.60 and the PPP results from GIPSY-OASIS II v6.3 software. In each column, R^2 values and hypothesis test results are given.

Hypothesis test results are based on a 95% confidence level. If the hypothesis H_0 is accepted, it is shown that there is no statistically significant difference from the geodetic site velocities from sub-sessions to those from 24h session results. If the hypothesis H_0 is rejected (only expressed in **bold**), the posteriori unit variance obtained from the least square estimation is statistically different from the 24h one based the F-test, that is, the models used for the geodetic velocity estimation are not equivalent. Furthermore, both the results expressed in **bold and underlined** indicate that the model is equivalent, but the deformation rate from 24-hour session is statistically different from the velocities from the sub-sessions based on the Student's t test.

In Fig. 2, the subplots of the horizontal component clearly show the character of the tectonic motion linearly. In this context, once Table 4 and 5 are examined, it is obviously seen that R^2 values estimated from all sessions are so close to 1 except for GUAM, KERG, USUD (in Table 4) and DAV1 (in Table 5). For instance, the motion in USUD is thought to be due to the postseismic relaxation.

Success rates of velocity estimation from PPP and relative positioning are illustrated in Fig. 3. There blue bars are for 8h- and orange bars are for 12h-sessions. With the success rate here, we mean the success of velocity estimation from short sessions when velocity estimation from 24h- is taken as the truth. Dashed pattern shows PPP results, whereas no pattern is for relative positioning. First of all, success rates for the horizontal components vary from 40 to 90%. Furthermore, the rates from 12h-sessions are higher than those of the 8h-sessions as expected. Note that the horizontal success rates from PPP are higher than those of the relative positioning, formed over long baselines to use in tectonic studies.

The fact that the accuracy of the vertical component is worse than that of the horizontal component is often expressed in the literature and in practice by many researchers. Therefore, the repeatabilities for this component are larger, and the seasonal effects are much more apparent than the horizontal ones. For this reason, the values of R^2 in Table 5 are much lower than those calculated from the horizontal component (around 0.40). Likewise, the results of the hypothesis test were rejected at a higher rate. Both for PPP and relative positioning, success rates for the vertical component are so low varying from about 5 to 15%. These rates are almost same for both methods.

Overall, the success rates of 12h- solutions are higher than those of 8h- solutions, the systematic effect acting on shorter sessions is varried and greater. For both positioning methods, the east component has greater success than the north one with regard to the truth. The success rates in Fig. 3 are higher for PPP than relative positioning because in the GAMIT/GLOBK processing are formed long baselines. Over long baselines, troposphere and ionosphere modelling become difficult, orbit errors accumulate, and hence ambiguity resolution becomes worse.

The reliability of velocity estimation from short GPS campaigns using PPP has been improved here when comparing results with those of Akarsu et. al. (2015). By the improvement we mean that the statistical agreement between the velocity estimated from short GPS observation and those of 24h sessions is higher here. The improvement in the horizontal component is 35% and 40% for 8h and 12h respectively. The vertical component was improved 4% and 17% for 8h and 12h respectively. This improvement might be ascribed to a few developments in the analysis procedures. First of all, here we used GPS time series spread over the years 2000 onwards. In other words, the noisier part 1990-2000 which might have affected the quality of estimated velocities in Akarsu et. al. (2015) is eliminated. Second, the analysis was performed with reprocessed orbits and clocks. JPL changed its orbit and clock estimation strategy as of the year 2007 (Hayal and Sanli, 2016). Third, GIPSY single receiver ambiguity resolution was further improved the accuracy of PPP (Bertiger et. al., 2010). Bertiger et. al. (2010) and Hayal and Sanli (2016) showed how positioning accuracy was improved with reprocessed JPL products and single receiver ambiguity resolution. Reprocessing especially improved the east component and this is correlated with the findings in this paper. Fourth, campaign measurements were performed in three consecutive days (i.e. the sampling was made such that IGS data were processed sellecting 3-consecutive days from the archive). Therefore, it was possible to eliminate the outlier solution from the processing. Finally, GPS campaigns were selected from the days in which the effect of geomagnetic storms is eliminated.

Eckl et. al. (2001) showed that using proper ambiguity resolution, troposphere modelling, and IGS precise orbits relative positioning performs uniformly, i.e. is not dependent on baseline length, for baseline lengths shorter than 300 km. In this experiment, GAMIT/GLOBK relative positioning used baselines longer than 300 km. This degraded the accuracy of positioning and hence the velocity estimation of relative positioning. This was even achieved with slightly coarser accuracy than the PPP positioning. Based on relative positioning, BERNESE processing also gave similar results in Duman and Sanli (2016). Many studies in the literature monitoring tectonics with long baselines to stable plates need to take this into account (Ayhan et. al., 2002; Aktuğ et. al., 2015; Reilinger et. al., 2006; Ozener et. al., 2010).

4 Conclusions

We incorporated relative positioning in the determination of the accuracy of GPS site velocities from GPS campaigns (i.e. Observation sessions shorter than 24 h). Relative positioning results were produced from GAMIT/GLOBK. The results were also compared with PPP solutions derived from GIPSY/OASIS II. A global experiment for proper sampling was adopted using the IGS network.

The results indicate that relative positioning using long baselines and short observation sessions produces similar results as with PPP. The accuracy is slightly coarser for horizontal positioning and slightly better for vertical positioning. Previously it has been noted that the accuracy of relative positioning does not depend on baseline length if baselines are shorter than 300 km. In the GAMIT/GLOBK processing here, reference points were chosen longer than 300 km.

It has also been noted that the accuracy of GPS site velocities derived from short observation sessions using PPP was improved here compared to previous studies. This is ascribed to the fact that the new GIPSY PPP runs with a new ambiguity resolution algorithm called single receiver ambiguity resolution. This especially improved the east component and the east results in this study show better accuracy. Furthermore, the analysis was performed using reprocessed JPL orbits and clocks. The contribution of JPL reprocessed products to positioning was previously discussed among researchers. Differing from the previous studies, our sampling here also comprises GPS days freed from the effect of geomagnetic storms. In addition, repeating campaign GPS measurements in three consecutive days helps removal of a bad solution from the analysis. The noisier IGS time series between 1990 and 2000 was not used. If the user takes into account the above listed factors in the planning of their field works they should expect similar types of accuracy levels.

In this study, the horizontal velocity accuracy of GPS campaigns with 12 h observation sessions from PPP seems to reach the confidence level of about 85%. However, the reliability of vertical velocities is very poor and about at 20% level. This means that tectonic studies trying to use the daylight as the observation duration would still produce poorer accuracy than the expected 95%. Of course this result is based on GPS solutions only, one should expect 95% levels once solutions are compiled from multi-GNSS experiments. Although the accuracy of velocity estimation was improved about 40% for horizontal and 20% for vertical positioning, it is still not at the desired confidence level.

Acknowledgements. The authors are grateful to the IGS for the distribution of GNSS data and to SOPAC for perfect archiving service of the data. The figures were plotted using "The Generic Mapping Tools" and we express our gratitude to the open source software designers.

~~References~~

Akarsu, V., Sanli, D., and Arslan, E.: Accuracy of velocities from repeated GPS measurements, Natural Hazards and Earth System Sciences, 15, 875-884, doi:10.5194/nhess-15-875-2015, 2015.

Aktuğ, B., Kiliçoğlu, A., Lenk, O., and Gürdal, M. A.: Establishment of regional reference frames for quantifying active deformation areas in Anatolia, Studia Geophysica et Geodaetica, 53, 169-183, doi: 10.1007/s11200-009-0011-0, 2009.

Aktuğ, B., Meherremov, E., Kurt, M., Özdemir, S., Esedov, N., and Lenk, O.: GPS constraints on the deformation of Azerbaijan and surrounding regions, Journal of Geodynamics, 67, 40-45, DOI: 10.1016/j.jog.2012.05.007, 2013.

Aktuğ, B., Doğru, A., Özener, H., and Peyret, M.: Slip rates and locking depth variation along central and easternmost segments of North Anatolian Fault, Geophysical Journal International, 202, 2133-2149, doi: 10.1093/gji/ggv274, 2015.

Altamimi, Z., Métivier, L., and Collilieux, X.: ITRF2008 plate motion model, Journal of Geophysical Research: Solid Earth, 117, B07402, doi:10.1029/2011JB008930, 2012.

Ayhan, M. E., Demir, C., Lenk, O., Kilicoglu, A., Altiner, Y., Barka, A. A., ... and Ozener, H.: Interseismic strain accumulation in the Marmara Sea region. Bulletin of the Seismological Society of America, 92(1), 216-229, 2002.

Bertiger, W., Desai, S. D., Haines, B., Harvey, N., Moore, A. W., Owen, S., and Weiss, J. P.: Single receiver phase ambiguity resolution with GPS data. Journal of Geodesy, 84(5), 327-337, 2010.

Blewitt, G., and Lavallée, D.: Effect of annual signals on geodetic velocity, Journal of Geophysical Research: Solid Earth, 107, 9-1 - 9-11, 2002.

Doğan, U.: Accuracy analysis of relative positions of permanent GPS stations in the Marmara region, Turkey, Survey Review, 39, 156-165, 2007.

Dogan, U., Demir, D. Ö., Çakir, Z., Ergintav, S., Ozener, H., Akoğlu, A. M., Nalbant, S. S., and Reilinger, R.: Postseismic deformation following the Mw 7.2, 23 October 2011 Van earthquake (Turkey): Evidence for aseismic fault reactivation, Geophysical Research Letters, 41, 2334-2341, 2014.

Dong, D., Herring, T., and King, R.: Estimating regional deformation from a combination of space and terrestrial geodetic data, Journal of Geodesy, 72, 200-214, 1998.

Duman, H., and Sanli, D. U., "Accuracy of velocities from repeated GPS surveys: relative positioning is concerned." EGU General Assembly Conference Abstracts. Vol. 18. 2016.

Eckl, M., Snay, R., Soler, T., Cline, M., and Mader, G.: Accuracy of GPS-derived relative positions as a function of interstation distance and observing-session duration, Journal of Geodesy, 75, 633-640, 2001.

Feigl, K. L., Agnew, D. C., Bock, Y., Dong, D., Donnellan, A., Hager, B. H., Herring, T. A., Jackson, D. D., Jordan, T. H., and King, R. W.: Space geodetic measurement of crustal deformation in central and southern California, 1984–1992, Journal of Geophysical Research: Solid Earth, 98, 21677-21712, 1993.

Firuzabadì, D., and King, R. W.: GPS precision as a function of session duration and reference frame using multi-point software, GPS solutions, 16, 191-196, 2012.

Floyd, M., Billiris, H., Paradissis, D., Veis, G., Avallone, A., Briole, P., McClusky, S., Nocquet, J. M., Palamartchouk, K., and Parsons, B.: A new velocity field for Greece: Implications for the kinematics and dynamics of the Aegean, Journal of Geophysical Research: Solid Earth, 115, B10403, 2010.

Hastaoglu, K., and Sanli, D.: Accuracy of GPS rapid static positioning: Application to Koyulhisar landslide, central Turkey, Survey Review, 43, 226-240, 2011.

Hayal, A. G., and Sanli, D. U.: Revisiting the role of observation session duration on precise point positioning accuracy using GIPSY/OASIS II Software. Boletim de Ciências Geodésicas, 22(3), 405-419, 2016.

Kenyeres, A., and Bruyninx, C.: EPN coordinate time series monitoring for reference frame maintenance, GPS solutions, 8, 200-209, 2004.

Koulali, A., Tregoning, P., McClusky, S., Stanaway, R., Wallace, L., and Lister, G.: New Insights into the present-day kinematics of the central and western Papua New Guinea from GPS, Geophysical Journal International, 202, 993-1004, 2015.

McClusky, S., Balassanian, S., Barka, A., Demir, C., Ergintav, S., Georgiev, I., Gurkan, O., Hamburger, M., Hurst, K., and Kahle, H.: Global Positioning System constraints on plate kinematics and dynamics in the eastern Mediterranean and Caucasus, Journal of Geophysical Research: Solid Earth, 105, 5695-5719, 2000.

Montillet, J.-P., Williams, S., Koulali, A., and McClusky, S.: Estimation of offsets in GPS time-series and application to the detection of earthquake deformation in the far-field, Geophysical Journal International, 200, 1207-1221, 2015.

Moore, M., Watson, C., King, M., McClusky, S., and Tregoning, P.: Empirical modelling of site-specific errors in continuous GPS data, Journal of Geodesy, 88, 887-900, 2014.

Müller, M., Geiger, A., Kahle, H.-G., Veis, G., Billiris, H., Paradissis, D., and Felekis, S.: Velocity and deformation fields in the North Aegean domain, Greece, and implications for fault kinematics, derived from GPS data 1993–2009, Tectonophysics, 597, 34-49, 2013.

Ozener, H., Arpat, E., Ergintav, S., Dogru, A., Cakmak, R., Turgut, B., and Dogan, U.: Kinematics of the eastern part of the North Anatolian Fault Zone, Journal of Geodynamics, 49, 141-150, 2010.

Reilinger, R., McClusky, S., Vernant, P., Lawrence, S., Ergintav, S., Cakmak, R., Ozener, H., Kadirov, F., Guliev, I., and Stepanyan, R.: GPS constraints on continental deformation in the Africa-Arabia-Eurasia continental collision zone and implications for the dynamics of plate interactions, Journal of Geophysical Research: Solid Earth, 111, B05411, 2006.

Ozener, H., Arpat, E., Ergintav, S., Dogru, A., Cakmak, R., Turgut, B., and Dogan, U.: Kinematics of the eastern part of the North Anatolian Fault Zone. Journal of geodynamics,49(3-4), 141-150, 2010.

Sanli, D. U., and Engin, C.: Accuracy of GPS positioning over regional scales, Survey Review, 41, 192-200, 2009.

Santamaría-Gómez, A., Bouin, M. N., Collilieux, X., and Wöppelmann, G.: Correlated errors in GPS position time series: implications for velocity estimates, Journal of Geophysical Research: Solid Earth, 116, B01405, 2011.

Segall, P., and Davis, J. L.: GPS applications for geodynamics and earthquake studies, Annual Review of Earth and Planetary Sciences, 25, 301-336, 1997

Soler, T., Michalak, P., Weston, N., Snay, R., and Foote, R.: Accuracy of OPUS solutions for 1-to 4-h observing sessions, GPS solutions, 10, 45-55, 2006.

Tatar, O., Poyraz, F., Gürsoy, H., Cakir, Z., Ergintav, S., Akpınar, Z., Koçbulut, F., Sezen, F., Türk, T., and Hastaoğlu, K. Ö.: Crustal deformation and kinematics of the Eastern Part of the North Anatolian Fault Zone (Turkey) from GPS measurements, Tectonophysics, 518, 55-62, 2012.

T.A. Herring, R.W. King, S. McClusky: Documentation For The GAMIT GPS Analysis Software, Massachusetts Institute of Technology, ABD, 2006.

T.A. Herring, R.W. King, S. McClusky: Documentation For The GLOBK GPS Analysis Software, Massachusetts Institute of Technology, ABD, 2006.

Zumberge, J., Heflin, M., Jefferson, D., Watkins, M., and Webb, F. H.: Precise point positioning for the efficient and robust analysis of GPS data from large networks, Journal of Geophysical Research: Solid Earth, 102, 5005-5017, 1997.

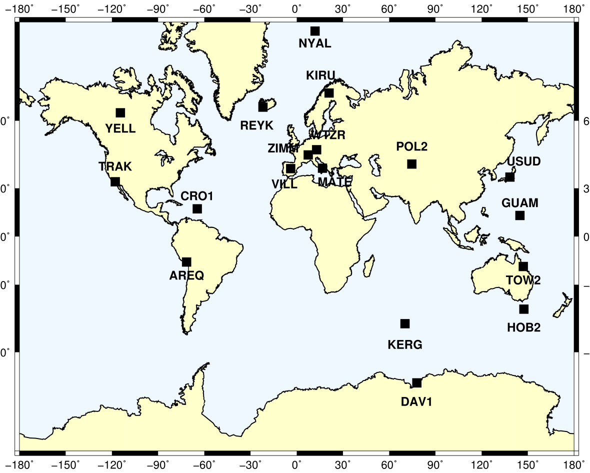

Figure 1. IGS continuous GPS sites used in the study.

Nat. Hazards Earth Syst. Sci. Discuss., https://doi.org/10.5194/nhess-2018-258
Manuscript under review for journal Nat. Hazards Earth Syst. Sci.
Discussion started: 19 October 2018

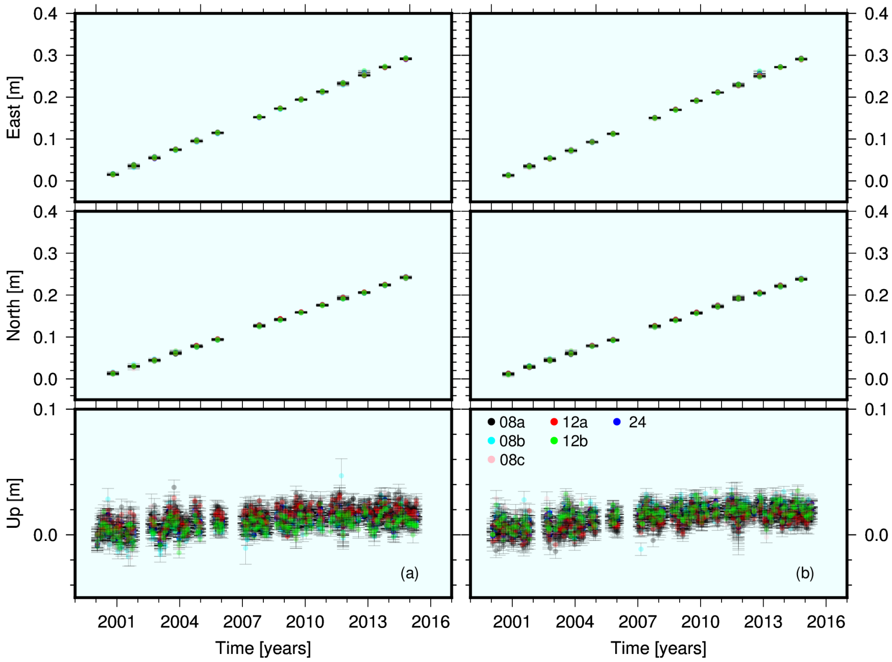

Figure 2. Time series of all sub-sessions for the site ZIMM from (a) relative positioning and (b) PPP solutions.

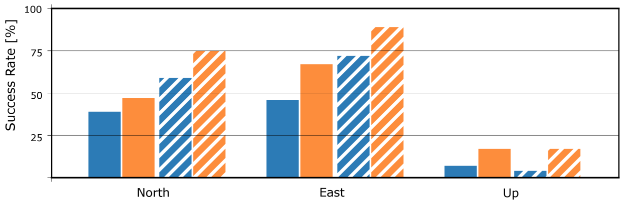

Figure 3. Success rates of 8h- and 12h-sessions. The velocity estimation from short sessions is compared with 24h results for each GPS component. Blue bars are for the 8h- and orange bars are for the 12h-sessions. Dashed patterns illustrate PPP estimates whereas no patterns are for the relative positioning.

Table 1. Segmented sub-sessions

Session Length	**Session Duration Times**		
[hours]	**a**	**b**	**c**
8	00:00 - 08:00	08:00 - 16:00	16:00 - 24:00
12	00:00 - 12:00	12:00 - 24:00	

Table 2. Site velocities and R^2 values from both solutions for the site ZIMM

GPS Baselines		**R^2 / Velocities [mm/yr]**					
Observation Sessions		**08a**	**08b**	**08c**	**12a**	**12b**	**24**
GAMIT/GLOBK	**East**	0.9998	0.9994	0.9998	0.9999	0.9995	0.9998
		19.58	19.73	19.85	19.65	19.82	19.76
	North	0.9997	0.9991	0.9994	0.9997	0.9995	0.9997
		16.25	16.21	16.29	16.34	16.21	16.28
	Up	0.4338	0.3095	0.2704	0.4099	0.3615	0.4714
		1.06	1.06	0.67	0.96	0.76	0.91
GIPSY/OASIS II	**East**	0.9997	0.9991	0.9996	0.9997	0.9994	0.9997
		19.69	19.77	19.78	19.73	19.77	19.75
	North	0.9996	0.9992	0.9989	0.9996	0.9991	0.9996
		16.16	16.10	16.11	16.17	16.04	16.11
	Up	0.4233	0.3174	0.3433	0.4324	0.4005	0.4900
		1.08	0.97	0.92	1.00	0.99	0.99

Table 3. For the north component, R^2 values and hypothesis test results for relative positioning and PPP

Stations	GAMIT/GLOBK v10.60					GIPSY/OASIS II v6.3				
	8 h		**12 h**		**24 h**	**8 h**		**12 h**		**24 h**
	R^2	**Test Results**	R^2	**Test Results**	R^2	R^2	**Test Results**	R^2	**Test Results**	R^2
AREQ	0.9816	H0 accepted	0.9810	H0 accepted	0.9811	0.9853	H0 accepted	0.9850	H0 accepted	0.9840
	0.9823	H0 accepted	0.9782	H0 accepted		0.9839	H0 accepted	0.9833	H0 accepted	
	0.9792	H0 accepted				0.9828	H0 accepted			
CRO1	0.9953	**H0 rejected**	0.9967	H0 accepted	0.9974	0.9980	H0 accepted	0.9980	H0 accepted	0.9984
	0.9926	**H0 rejected**	0.9966	H0 accepted		0.9970	**H0 rejected**	0.9968	**H0 rejected**	
	0.9960	H0 accepted				0.9975	H0 accepted			
DAV1	0.9883	**H0 rejected**	0.9915	**H0 rejected**	0.9803	0.9817	H0 accepted	0.9847	H0 accepted	0.9825
	0.9825	**H0 rejected**	0.9756	H0 accepted		0.9804	H0 accepted	0.9744	H0 accepted	
	0.9720	H0 accepted				0.9718	H0 accepted			
GUAM	0.7315	H0 accepted	0.7835	H0 accepted	0.7817	0.8922	H0 accepted	0.9037	H0 accepted	0.9020
	0.8178	H0 accepted	0.7880	**H0 rejected**		0.9168	H0 accepted	0.8759	H0 accepted	
	0.7830	H0 accepted				0.8702	H0 accepted			
HOB2	0.9998	**H0 rejected**	0.9999	H0 accepted	0.9999	0.9999	**H0 rejected**	0.9999	**H0 rejected**	0.9999
	0.9998	**H0 rejected**	0.9998	**H0 rejected**		0.9999	H0 accepted	0.9999	H0 accepted	
	0.9998	**H0 rejected**				0.9999	**H0 rejected**			
KERG	0.7352	**H0 rejected**	0.7891	**H0 rejected**	0.8809	0.8324	H0 accepted	0.8298	H0 accepted	0.8766
	0.8470	H0 accepted	0.8152	H0 accepted		0.8457	H0 accepted	0.8423	**H0 rejected**	
	0.8121	**H0 rejected**				0.7685	**H0 rejected**			
KIRU	0.9992	**H0 rejected**	0.9994	**H0 rejected**	0.9993	0.9991	H0 accepted	0.9991	H0 accepted	0.9991
	0.9989	**H0 rejected**	0.9992	H0 accepted		0.9985	**H0 rejected**	0.9987	H0 accepted	
	0.9992	**H0 rejected**				0.9990	**H0 rejected**			
MATE	0.9995	**H0 rejected**	0.9996	**H0 rejected**	0.9998	0.9994	**H0 rejected**	0.9995	H0 accepted	0.9997
	0.9996	**H0 rejected**	0.9995	**H0 rejected**		0.9992	**H0 rejected**	0.9994	**H0 rejected**	
	0.9993	**H0 rejected**				0.9991	**H0 rejected**			
NYAL	0.9981	**H0 rejected**	0.9981	**H0 rejected**	0.9989	0.9992	H0 accepted	0.9992	H0 accepted	0.9993
	0.9979	**H0 rejected**	0.9988	H0 accepted		0.9990	H0 accepted	0.9988	**H0 rejected**	
	0.9980	**H0 rejected**				0.9988	**H0 rejected**			
POL2	0.9797	**H0 rejected**	0.9755	**H0 rejected**	0.9841	0.9885	**H0 rejected**	0.9902	H0 accepted	0.9900
	0.9851	H0 accepted	0.9855	**H0 rejected**		0.9855	H0 accepted	0.9879	H0 accepted	
	0.9832	**H0 rejected**				0.9834	**H0 rejected**			
REYK	0.9993	H0 accepted	0.9994	**H0 rejected**	0.9994	0.9992	**H0 rejected**	0.9994	H0 accepted	0.9996
	0.9991	H0 accepted	0.9992	H0 accepted		0.9995	H0 accepted	0.9995	H0 accepted	
	0.9991	H0 accepted				0.9993	H0 accepted			
TOW2	0.9992	**H0 rejected**	0.9996	H0 accepted	0.9996	0.9998	**H0 rejected**	0.9998	**H0 rejected**	0.9999
	0.9995	**H0 rejected**	0.9996	**H0 rejected**		0.9999	H0 accepted	0.9999	H0 accepted	
	0.9996	H0 accepted				0.9999	**H0 rejected**			
TRAK	0.9970	H0 accepted	0.9976	H0 accepted	0.9969	0.9982	**H0 rejected**	0.9961	**H0 rejected**	0.9993
	0.9931	**H0 rejected**	0.9926	**H0 rejected**		0.9972	**H0 rejected**	0.9993	H0 accepted	
	0.9920	**H0 rejected**				0.9986	**H0 rejected**			
USUD	0.8624	H0 accepted	0.9008	H0 accepted	0.9162	0.9436	H0 accepted	0.9470	H0 accepted	0.9456
	0.9182	H0 accepted	0.8921	**H0 rejected**		0.9365	H0 accepted	0.9400	H0 accepted	
	0.8852	H0 accepted				0.9402	H0 accepted			
VILL	0.9990	**H0 rejected**	0.9992	**H0 rejected**	0.9995	0.9983	H0 accepted	0.9987	H0 accepted	0.9989
	0.9992	**H0 rejected**	0.9997	H0 accepted		0.9987	H0 accepted	0.9988	H0 accepted	
	0.9993	H0 accepted				0.9983	H0 accepted			
WTZR	0.9995	**H0 rejected**	0.9996	**H0 rejected**	0.9998	0.9994	H0 accepted	0.9995	H0 accepted	0.9996
	0.9994	**H0 rejected**	0.9997	**H0 rejected**		0.9985	**H0 rejected**	0.9995	H0 accepted	
	0.9997	H0 accepted				0.9995	H0 accepted			
YELL	0.9940	**H0 rejected**	0.9958	H0 accepted	0.9953	0.9970	H0 accepted	0.9973	H0 accepted	0.9970
	0.9923	**H0 rejected**	0.9912	**H0 rejected**		0.9961	H0 accepted	0.9937	**H0 rejected**	
	0.9879	**H0 rejected**				0.9921	**H0 rejected**			
ZIMM	0.9997	H0 accepted	0.9997	H0 accepted	0.9997	0.9996	H0 accepted	0.9996	H0 accepted	0.9996
	0.9991	**H0 rejected**	0.9995	**H0 rejected**		0.9992	**H0 rejected**	0.9991	**H0 rejected**	
	0.9994	**H0 rejected**				0.9989	**H0 rejected**			

Table 4. For the east, R^2 values and hypothesis test results for relative positioning and PPP.

Stations	GAMIT/GLOBK v10.60					GIPSY/OASIS II v6.3				
	8 h		**12 h**		**24 h**	**8 h**		**12 h**		**24 h**
	R^2	**Test Results**	R^2	**Test Results**	R^2	R^2	**Test Results**	R^2	**Test Results**	R^2
AREQ	0.9825	H0 accepted	0.9815	H0 accepted	0.9817	0.9870	H0 accepted	0.9875	H0 accepted	0.9882
	0.9835	H0 accepted	0.9808	H0 accepted		0.9883	H0 accepted	0.9888	H0 accepted	
	0.9816	H0 accepted				0.9888	H0 accepted			
CRO1	0.9935	H0 accepted	0.9945	H0 accepted	0.9944	0.9897	H0 accepted	0.9920	H0 accepted	0.9944
	0.9892	**H0 rejected**	0.9925	**H0 accepted**		0.9940	H0 accepted	0.9808	**H0 rejected**	
	0.9930	H0 accepted				0.9909	H0 accepted			
DAV1	0.8492	H0 accepted	0.9085	H0 accepted	0.9065	0.9745	H0 accepted	0.9776	H0 accepted	0.9801
	0.9139	**H0 rejected**	0.9241	H0 accepted		0.9746	H0 accepted	0.9619	**H0 rejected**	
	0.8434	**H0 rejected**				0.9521	**H0 rejected**			
GUAM	0.9902	**H0 rejected**	0.9892	H0 accepted	0.9916	0.9916	H0 accepted	0.9912	H0 accepted	0.9941
	0.9872	H0 accepted	0.9885	H0 accepted		0.9906	H0 accepted	0.9942	H0 accepted	
	0.9877	**H0 rejected**				0.9931	**H0 rejected**			
HOB2	0.9985	**H0 rejected**	0.9989	**H0 rejected**	0.9995	0.9971	**H0 rejected**	0.9983	H0 accepted	0.9988
	0.9984	**H0 rejected**	0.9992	H0 accepted		0.9985	H0 accepted	0.9985	H0 accepted	
	0.9967	**H0 rejected**				0.9978	**H0 rejected**			
KERG	0.9161	**H0 rejected**	0.9546	H0 accepted	0.9521	0.9695	H0 accepted	0.9684	H0 accepted	0.9702
	0.9618	**H0 rejected**	0.9464	H0 accepted		0.9669	H0 accepted	0.9683	H0 accepted	
	0.9381	H0 accepted				0.9607	**H0 rejected**			
KIRU	0.9994	**H0 rejected**	0.9995	**H0 rejected**	0.9995	0.9987	H0 accepted	0.9989	H0 accepted	0.9990
	0.9994	**H0 rejected**	0.9994	H0 accepted		0.9989	H0 accepted	0.9989	H0 accepted	
	0.9987	**H0 rejected**				0.9988	H0 accepted			
MATE	0.9997	**H0 rejected**	0.9998	H0 accepted	0.9999	0.9997	H0 accepted	0.9997	H0 accepted	0.9998
	0.9995	**H0 rejected**	0.9997	**H0 rejected**		0.9997	H0 accepted	0.9997	H0 accepted	
	0.9998	**H0 rejected**				0.9995	**H0 rejected**			
NYAL	0.9989	**H0 rejected**	0.9993	H0 accepted	0.9993	0.9988	H0 accepted	0.9989	H0 accepted	0.9990
	0.9987	**H0 rejected**	0.9996	H0 accepted		0.9982	**H0 rejected**	0.9988	H0 accepted	
	0.9988	H0 accepted				0.9976	**H0 rejected**			
POL2	0.9987	**H0 rejected**	0.9986	**H0 rejected**	0.9993	0.9991	H0 accepted	0.9993	H0 accepted	0.9993
	0.9993	H0 accepted	0.9992	H0 accepted		0.9994	H0 accepted	0.9993	H0 accepted	
	0.9993	H0 accepted				0.9990	H0 accepted			
REYK	0.9965	**H0 rejected**	0.9977	H0 accepted	0.9974	0.9960	H0 accepted	0.9974	H0 accepted	0.9974
	0.9962	H0 accepted	0.9964	H0 accepted		0.9976	H0 accepted	0.9964	H0 accepted	
	0.9946	**H0 rejected**				0.9962	H0 accepted			
TOW2	0.9994	H0 accepted	0.9995	**H0 rejected**	0.9996	0.9996	H0 accepted	0.9996	H0 accepted	0.9997
	0.9994	H0 accepted	0.9997	H0 accepted		0.9996	H0 accepted	0.9997	H0 accepted	
	0.9989	**H0 rejected**				0.9996	H0 accepted			
TRAK	0.9996	H0 accepted	0.9996	H0 accepted	0.9995	0.9993	**H0 rejected**	0.9995	H0 accepted	0.9997
	0.9994	H0 accepted	0.9995	H0 accepted		0.9993	**H0 rejected**	0.9997	H0 accepted	
	0.9992	H0 accepted				0.9978	**H0 rejected**			
USUD	0.9811	H0 accepted	0.9810	H0 accepted	0.9814	0.9790	H0 accepted	0.9824	H0 accepted	0.9826
	0.9836	H0 accepted	0.9826	H0 accepted		0.9826	H0 accepted	0.9826	H0 accepted	
	0.9827	H0 accepted				0.9796	H0 accepted			
VILL	0.9996	H0 accepted	0.9997	H0 accepted	0.9997	0.9995	H0 accepted	0.9996	H0 accepted	0.9996
	0.9994	**H0 rejected**	0.9996	**H0 rejected**		0.9993	**H0 rejected**	0.9996	H0 accepted	
	0.9996	H0 accepted				0.9995	H0 accepted			
WTZR	0.9995	**H0 rejected**	0.9996	**H0 rejected**	0.9998	0.9993	**H0 rejected**	0.9995	H0 accepted	0.9997
	0.9997	**H0 rejected**	0.9998	H0 accepted		0.9996	H0 accepted	0.9998	H0 accepted	
	0.9998	H0 accepted				0.9997	H0 accepted			
YELL	0.9970	**H0 rejected**	0.9985	**H0 rejected**	0.9965	0.9979	H0 accepted	0.9983	H0 accepted	0.9986
	0.9975	H0 accepted	0.9933	**H0 rejected**		0.9987	H0 accepted	0.9966	**H0 rejected**	
	0.9891	**H0 rejected**				0.9897	**H0 rejected**			
ZIMM	0.9998	**H0 rejected**	0.9999	**H0 rejected**	0.9998	0.9997	H0 accepted	0.9997	H0 accepted	0.9997
	0.9994	**H0 rejected**	0.9995	**H0 rejected**		0.9991	**H0 rejected**	0.9994	**H0 rejected**	
	0.9998	H0 accepted				0.9996	H0 accepted			

Table 5. For the up, R^2 values and hypothesis test results for relative positioning and PPP.

Stations	**GAMIT/GLOBK v10.60**					**GIPSY/OASIS II v6.3**				
	8 h		**12 h**		**24 h**	**8 h**		**12 h**		**24 h**
	R^2	**Test Results**	R^2	**Test Results**	R^2	R^2	**Test Results**	R^2	**Test Results**	R^2
AREQ	0.2631	**H0 rejected**	0.2216	**H0 rejected**	0.3542	0.4916	**H0 rejected**	0.5595	H0 accepted	0.5372
	0.2445	**H0 rejected**	0.1730	**H0 rejected**		0.4303	**H0 rejected**	0.4172	**H0 rejected**	
	0.1148	**H0 rejected**				0.3689	**H0 rejected**			
CRO1	0.3195	**H0 rejected**	0.3316	**H0 rejected**	0.4295	0.2017	**H0 rejected**	0.2893	**H0 rejected**	0.4269
	0.3564	**H0 rejected**	0.2437	**H0 rejected**		0.2525	**H0 rejected**	0.2026	**H0 rejected**	
	0.2114	**H0 rejected**				0.2185	**H0 rejected**			
DAV1	0.2535	**H0 rejected**	0.2231	**H0 rejected**	0.2382	0.2246	**H0 rejected**	0.3060	**H0 rejected**	0.2259
	0.1533	**H0 rejected**	0.1747	**H0 rejected**		0.2042	**H0 rejected**	0.0599	**H0 rejected**	
	0.1072	**H0 rejected**				0.0528	**H0 rejected**			
GUAM	0.1177	**H0 rejected**	0.1343	**H0 rejected**	0.1125	0.0513	**H0 rejected**	0.0490	**H0 rejected**	0.0571
	0.0462	**H0 rejected**	0.0999	**H0 rejected**		0.0184	**H0 rejected**	0.0469	**H0 rejected**	
	0.1015	**H0 rejected**				0.0427	**H0 rejected**			
HOB2	0.0387	**H0 rejected**	0.0282	**H0 rejected**	0.0546	0.1889	**H0 rejected**	0.2199	**H0 rejected**	0.2894
	0.0615	**H0 rejected**	0.0620	**H0 rejected**		0.1836	**H0 rejected**	0.1611	**H0 rejected**	
	0.0567	**H0 rejected**				0.0958	**H0 rejected**			
KERG	0.2870	**H0 rejected**	0.3320	**H0 rejected**	0.4723	0.0932	**H0 rejected**	0.1247	**H0 rejected**	0.1993
	0.3759	**H0 rejected**	0.4180	**H0 rejected**		0.0992	**H0 rejected**	0.1478	**H0 rejected**	
	0.3579	**H0 rejected**				0.1337	**H0 rejected**			
KIRU	0.8169	H0 accepted	0.8241	H0 accepted	0.8174	0.8280	H0 accepted	0.8331	H0 accepted	0.8425
	0.7776	H0 accepted	0.7961	H0 accepted		0.8169	**H0 rejected**	0.8185	H0 accepted	
	0.7893	H0 accepted				0.8184	H0 accepted			
MATE	0.2250	**H0 rejected**	0.1726	**H0 rejected**	0.2347	0.0930	**H0 rejected**	0.1125	**H0 rejected**	0.2044
	0.1861	**H0 rejected**	0.2603	**H0 rejected**		0.1218	**H0 rejected**	0.1824	**H0 rejected**	
	0.1653	**H0 rejected**				0.1254	**H0 rejected**			
NYAL	0.9689	**H0 rejected**	0.9691	**H0 rejected**	0.9783	0.9628	**H0 rejected**	0.9646	**H0 rejected**	0.9733
	0.9547	**H0 rejected**	0.9673	**H0 rejected**		0.9518	**H0 rejected**	0.9635	**H0 rejected**	
	0.9612	**H0 rejected**				0.9584	**H0 rejected**			
POL2	0.3080	**H0 rejected**	0.2624	**H0 rejected**	0.3324	0.2000	**H0 rejected**	0.1977	**H0 rejected**	0.2095
	0.1290	**H0 rejected**	0.3037	**H0 rejected**		0.1167	**H0 rejected**	0.1575	**H0 rejected**	
	0.2513	**H0 rejected**				0.1790	**H0 rejected**			
REYK	0.2590	**H0 rejected**	0.2774	H0 accepted	0.2492	0.2705	**H0 rejected**	0.3187	H0 accepted	0.3112
	0.2942	**H0 rejected**	0.2525	**H0 rejected**		0.3359	**H0 rejected**	0.2428	**H0 rejected**	
	0.2324	**H0 rejected**				0.1716	**H0 rejected**			
TOW2	0.3345	**H0 rejected**	0.2440	**H0 rejected**	0.3889	0.5033	**H0 rejected**	0.5034	**H0 rejected**	0.5657
	0.1781	**H0 rejected**	0.3598	**H0 rejected**		0.3938	**H0 rejected**	0.4722	**H0 rejected**	
	0.3405	**H0 rejected**				0.4446	**H0 rejected**			
TRAK	0.2662	**H0 rejected**	0.2262	**H0 rejected**	0.2887	0.2370	**H0 rejected**	0.3055	**H0 rejected**	0.3646
	0.0784	**H0 rejected**	0.2334	**H0 rejected**		0.3616	**H0 rejected**	0.2880	**H0 rejected**	
	0.3202	**H0 rejected**				0.2040	**H0 rejected**			
USUD	0.3990	**H0 rejected**	0.4883	**H0 rejected**	0.5123	0.4952	**H0 rejected**	0.5507	**H0 rejected**	0.5685
	0.4516	**H0 rejected**	0.5359	H0 accepted		0.5178	**H0 rejected**	0.4920	H0 accepted	
	0.5662	H0 accepted				0.4842	**H0 rejected**			
VILL	0.1156	**H0 rejected**	0.1620	**H0 rejected**	0.2615	0.3436	**H0 rejected**	0.4192	**H0 rejected**	0.4938
	0.1169	**H0 rejected**	0.2393	**H0 rejected**		0.3105	**H0 rejected**	0.3591	**H0 rejected**	
	0.2488	**H0 rejected**				0.2690	**H0 rejected**			
WTZR	0.3145	**H0 rejected**	0.4220	**H0 rejected**	0.4262	0.2357	**H0 rejected**	0.3047	**H0 rejected**	0.3060
	0.3689	**H0 rejected**	0.3815	**H0 rejected**		0.2412	**H0 rejected**	0.2306	**H0 rejected**	
	0.3281	**H0 rejected**				0.2087	**H0 rejected**			
YELL	0.9095	**H0 rejected**	0.9272	H0 accepted	0.9362	0.9287	**H0 rejected**	0.9394	**H0 rejected**	0.9494
	0.9106	**H0 rejected**	0.9274	H0 accepted		0.9340	**H0 rejected**	0.9449	H0 accepted	
	0.9090	**H0 rejected**				0.9369	**H0 rejected**			
ZIMM	0.4338	**H0 rejected**	0.4099	**H0 rejected**	0.4714	0.4233	**H0 rejected**	0.4324	**H0 rejected**	0.4900
	0.3095	**H0 rejected**	0.3615	**H0 rejected**		0.3174	**H0 rejected**	0.4005	**H0 rejected**	
	0.2704	**H0 rejected**				0.3433	**H0 rejected**			